Magnetic Dynamos and Magnetic Helicity Transport: General Principles and Astrophysical Implications

(Eric G. Blackman, Univ. of Rochester)

- Magnetic fields: observed entities and intermediary between gravity and radiation
- Sun, stars, galaxies, and accretion disks have large magnetic Reynolds numbers, are turbulent.
- Understanding the magnetic spectrum of these systems requires understanding MHD turbulence and dynamo theory.
- Semi-analytic calculations and numerical experiments play symbiotic role: numerical simulations alone are not enough

Consider forced turbulence: Divide the spectrum into two regimes

Small Scale Fields:

- Fields ordered at or below the input scale, extending all the way to the smaller of the viscous or resistive cutoff scale.
- **small scale dynamo**

Large Scale Field:

- Field ordered on scales larger than that of the input turbulence
- **mean field dynamo**, shear amplification

SPECTRAL VIEW OF IN SITU AMPLIFICATION

- Ultimately want to understand the shape of this curve
- Note the distinction between regions $k < k_{input}$ and $k > k_{input}$.

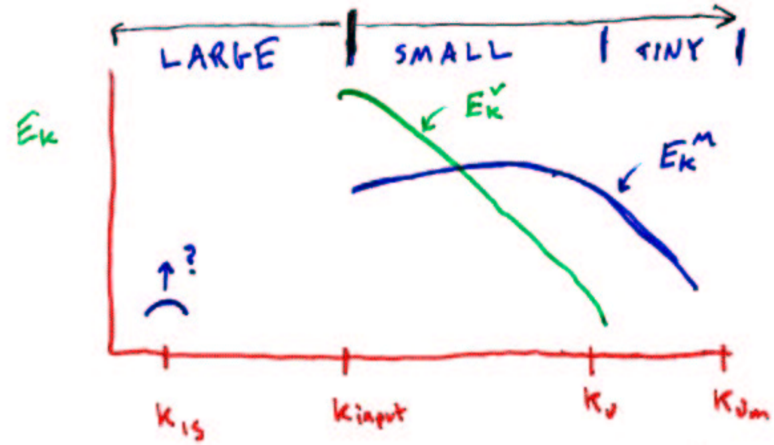

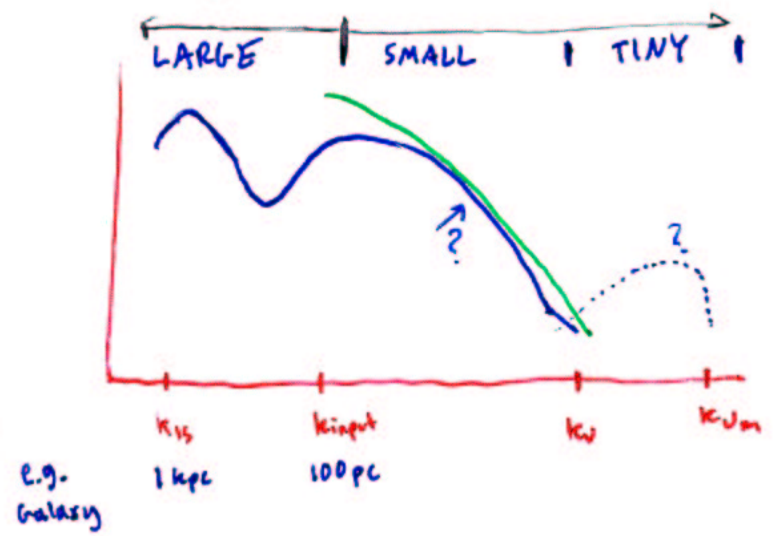

IN SITU AMPLIFICATION (small scale fields)

Turbulent Amplification/ Small Scale Dynamo

- B-energy grows to near equipartition with v-energy
- Helicity not required for exponential growth, but matters for location of spectral peak
- "classic non-helical picture" (e.g. Kulsrud & Anderson) B peaks on scale of input turbulence: grows on smallest scale first then "locally inverse cascades" up to input scale.
- "revised non-helical picture" (e.g. Kida et al. '91 Maron & Cowley '01) B grows only for $\nu_m < \nu_v$ and peaks on resistive scale: large scale motions directly input energy into smallest scales and create magnetic folds with small cross field gradient scales.
- "helical picture" (e.g. Maron and Blackman '02) B grows only for $\nu_{mag} < \nu_{kin}$ but peak moves to input scale for $f_h > f_{h,crit}$.
- e.g. supernova turbulence, input scale 50-100pc
- random walk growth/field line stretching

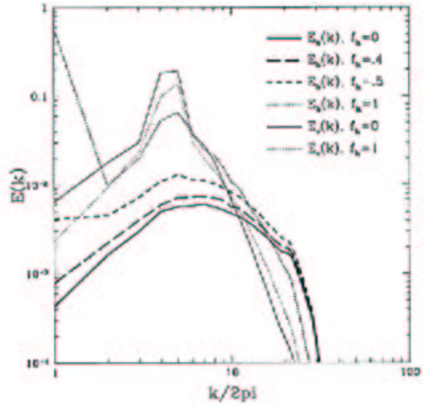

Figure 1: Saturated kinetic and magnetic energy spectra for values of f_h (MB 02).

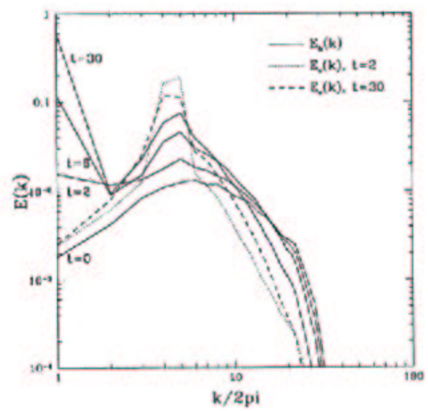

Figure 2: Time sequence of v and B energy spectra for $f_h = 1$. (MB 02; also Meneguzzi et al. '81; Brandenburg '01)

IN SITU AMPLIFICATION (large scale fields)

1. **Mean Field Dynamo (MFD)** → exponential growth

- **B** grows on scales > forcing scales
- "α-helicity" involved in growth: forcing with finite $\langle \mathbf{v} \cdot \nabla \times \mathbf{v} \rangle$
- involves turbulence + rotation + density gradient
- also requires "turbulent diffusion coefficient β" for **net flux**
- can account for fast changes in large scale **B**
- growth rate longer than for "small scale dynamo"
- spatial mean ~ ensemble mean for 2 scaled systems
- controversial: are α and β prematurely quenched? e.g. is MFD FAST or SLOW?

MFD: simple framework for understanding the inverse cascade of magnetic helicity in turbulent flows.

2. **Shear+MRI**="Ω" effect→ simple linear stretching of exponentially sustained small scale field can produce exponential growth of large scale field–but no flux produced.

For the Galaxy:

Small Scale Field:

- random, 5μG; scale ~ few 50-100pc (outer)
- near equipartition between field and random kinetic motions on the scale of the input turbulence.
- not sure how well we know the structure of the field on all scales though..

Large Scale Field:

- toroidal outside 200pc
- few μG; scale $\gtrsim$ few kpc, reversals
- poloidal inside 200pc; 10^{-3}G
- To what extent is the large scale field produced in situ?
- Do large scale field dynamos operate FAST (growth rate independent of R_m or SLOW (growth rate decreases with R_m)?

Note also: (1) Prandtl number $\equiv \nu_v/\nu_m >> 1$ for Galaxy

Note also: (2) Kinetic spectrum is observed to be Kolmogorov down to about $\gtrsim 10^9$cm.

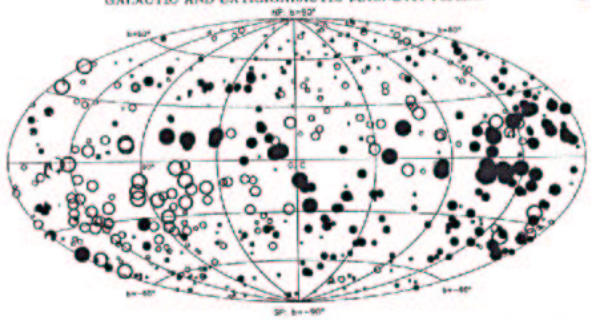

Figure 3. The distribution of the *RMs* of extragalactic radio sources. Filled circles indicate positive *RMs*, open circles negative *RMs*. The area of the circles is proportional to $|RM|$ within limits of 5 and 150 rad/m^2 (from Han *et al.*, 1997).

Figure 2 shows the distribution of *RMs* of low-latitude pulsars, projected onto the Galactic plane, and the bisymmetric model by Han *et al.* (1999a). Some data disagree with the model. This may be due to local disturbances of the field e.g. by supernova remnants (Vallée, 1996), or the model is too simple. More pulsar *RM* data are needed to obtain a better sampling of the field structure. (c) Nonlinear dynamo models revealed a mixture of magnetic modes, while the dominance of the bisymmetric mode is very difficult to obtain. A model based on the rotation curve of M51 and a spiral modulation generated a large-scale reversal near the corotation radius in one half of the galaxy where the bisymmetric field can be trapped by the spiral pattern over the galaxy's lifetime (Bykov *et al.*, 1997, see below). However, no reversals at other radii appeared. (d) Large-scale anisotropic field loops may be produced by stretching or compressing (see below).

In external galaxies, data sampling is much denser than in the Galaxy. High-resolution maps of Faraday rotation, which measure the *RMs* of the diffuse polarized synchrotron emission, are available for a couple of spiral galaxies (Beck *et al.*, 1996; Beck, 2000). It is striking that *only very few field reversals* have been detected in spiral galaxies where the spatial resolution is better than 1 kpc. The observed disk field of M51 can be described by a mixture of axisymmetric and bisymmetric components which may mimic a reversal for an observer located within the disk (see Figure 8a in Berkhuijsen *et al.*, 1997, compare with Figure 6 in Bykov *et al.*, 1997). In NGC 2997 a reversal between the disk field and the central region occurs at about 2 kpc

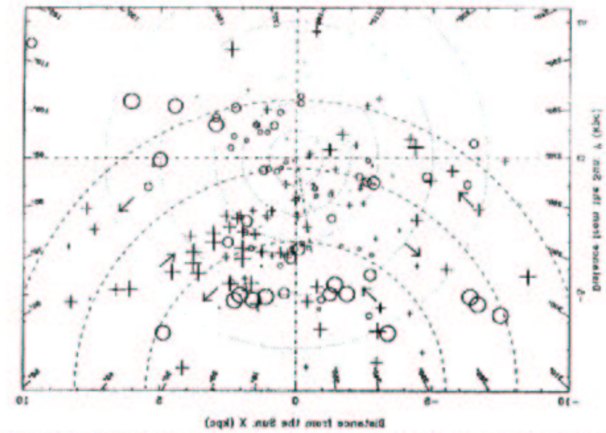

Figure 7. Distribution of pulsar RMs and the concentric-ring model sketched according to Rand & Kulkarni (1989) and Rand & Lyne (1994). Field directions expected for this model are indicated by arrows, and the dashed circles show where the field lines reverse. The dotted circles indicate equal distances from the Sun.

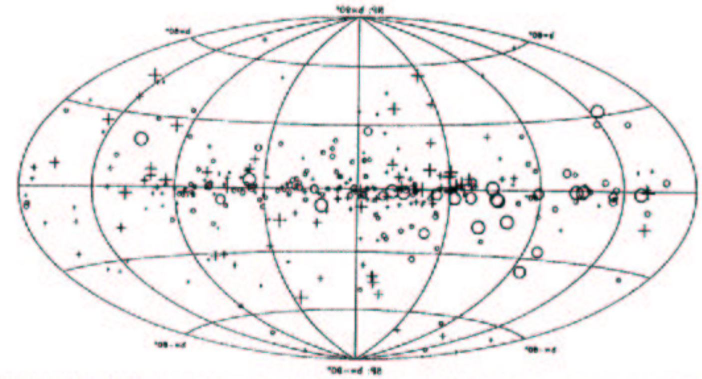

Figure 8. Distribution of $\langle B_\parallel \rangle$ of all measured pulsar RMs in Galactic coordinates. Plus signs indicate that the average field is directed towards us, and circles indicate that the average field is directed away from us. The size of symbols is proportional to the field strength within limits of 0.8 and 2.5 μG.

ordered magnetic fields in early epochs of galaxy formation (Udomprasert et al. 1997; Athreya et al. 1998), but dynamo processes (Kulsrud 1997; Parker 1997) will very likely amplify and modify the field structure. More realistic simulations (e.g. Bykov et al. 1997; Rohde & Elstner 1998) show wide variations in the form of the large-scale field. Furthermore, the field structure can be complicated by spiral streaming (Lou & Fan 1998; Moss 1998), stellar wind bubbles and supernova events. It is not surprising that the observed field structure in galactic discs cannot yet be fully explained by dynamo models (see the reviews by Kronberg 1994 and Beck et al. 1996).

6 CONCLUSIONS

In this paper we present RMs for 63 pulsars, 54 of which have no previously published RM data. RMs of three pulsars are shown to

Solar Field

- mean field $\simeq$ few G
- spots & loops $\gtrsim$ kG
- 22 year cycle =>
  - turbulent diffusion
  - shear
  - buoyancy of loops
  - "twist"
- Interface models

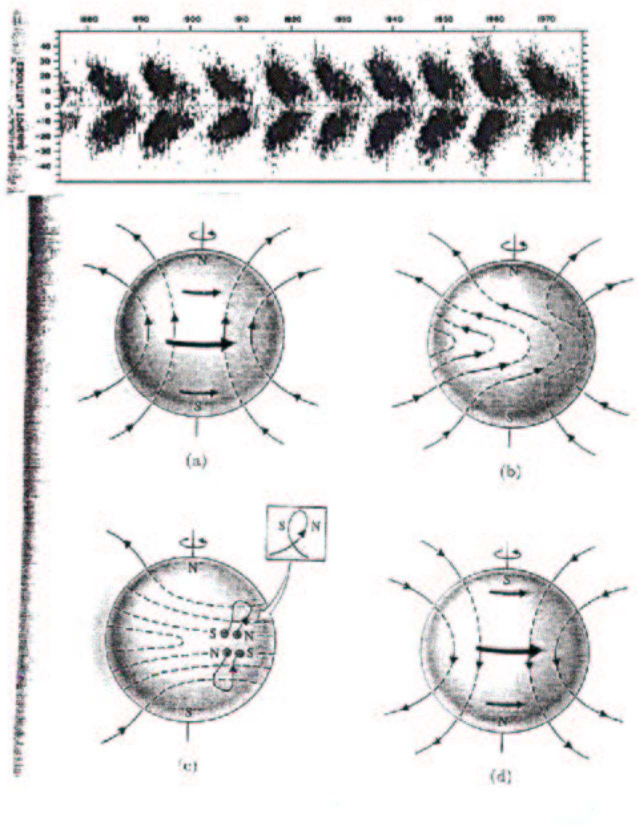

Basic Idea of Dynamo (mean field) e.g. Parker '59

"mean" large scale field growth requires

- helicity $\langle \vec{v} \cdot \vec{\omega} \rangle$
- turbulent diffusion of mean field } give exponential growth

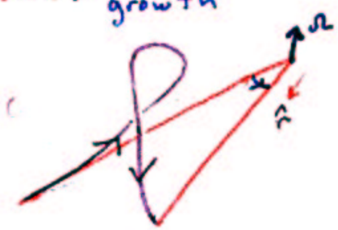

blob expands as rises in density gradient: gives vertical field component.

(1)

field twists clockwise: opposite to underlying rotation => radial field component

(2)

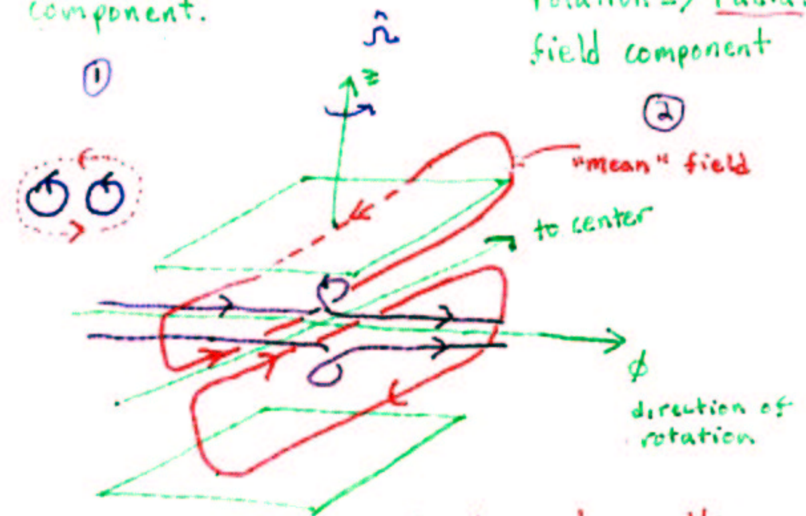

- mean flux within boundaries only results if top and bottom loops diffuse
- differential rotation stretches "poloidal" (r,z) field into "toroidal" (ϕ) field

MFD BASIC EQUATIONS AND BACKREATION

Write $\mathbf{V} = \mathbf{v} + \overline{\mathbf{V}}$ and $\mathbf{B} = \mathbf{b} + \overline{\mathbf{B}}$, then

$$\partial_t \overline{\mathbf{B}} = \nabla \times \langle \mathbf{v} \times \mathbf{b} \rangle + \nabla \times (\overline{\mathbf{V}} \times \overline{\mathbf{B}}),$$

$$\overline{\mathbf{E}} = \langle \mathbf{v} \times \mathbf{b} \rangle = \alpha \overline{\mathbf{B}} - \beta \nabla \times \overline{\mathbf{B}}$$

$$\alpha = -\tau_c[\langle \mathbf{v} \cdot \nabla \times \mathbf{v} \rangle - \langle \mathbf{b} \cdot \nabla \times \mathbf{b} \rangle]/3 = \alpha_0 + \alpha_m$$

$$\beta = \tau_c[\langle \mathbf{v} \cdot \mathbf{v} \rangle + \langle \mathbf{b} \cdot \mathbf{b} \rangle]/3 \ \ (?)$$

- **Kinematic theory**: no correction terms in b to α, β, $v = v^{(0)}$.
- **Backreaction**: might even a weak $\overline{B}$ and large b shut down field growth leading to SLOW MFD or NO MFD?
- Coefficients of the following form, if true for all times, would kill the MFD $\alpha \simeq \frac{\alpha_0}{(1+R_{M,2}\overline{\mathbf{B}}^2/\mathbf{b}^2)}$
- Revival of this concern in the 90s, (but has been around since Cowling 1957).
- Numerical simulations help but care is required in interpretation.
- **Dynamical** backreaction for simplest dynamo in a periodic box is now "nearly" understood(!): Numerical simulations of α^2 dynamo by Brandenburg (2001) can been explained semi-analytically (Field & Blackman 2002 and Blackman 2002; also w/Brandenburg 2002).
- Need to fully understand simplest, time-dependent theory even if periodic boundaries are unphysical →

ROLE OF MAGNETIC HELICITY

- $H_k \equiv \langle \mathbf{A} \cdot \mathbf{B} \rangle_k$. $E_k \geq |k H_k|$.

$$\tfrac{1}{2c}\partial_t \langle \overline{\mathbf{A}} \cdot \overline{\mathbf{B}} \rangle = -\langle \overline{\mathbf{E}} \cdot \overline{\mathbf{B}} \rangle = \langle \alpha \overline{B}^2 \rangle - (\nu_M + \beta)\langle \overline{\mathbf{J}} \cdot \overline{\mathbf{B}} \rangle + \nabla \cdot \langle .. \rangle$$

$$\tfrac{1}{2c}\partial_t \langle \mathbf{A} \cdot \mathbf{B} \rangle = -\langle \overline{\mathbf{E}} \cdot \overline{\mathbf{B}} \rangle - \langle \mathbf{e} \cdot \mathbf{b} \rangle = -\nu_M \langle \mathbf{J} \cdot \mathbf{B} \rangle + \nabla \cdot \langle .. \rangle$$

Two-Scale Approach:

$$\partial_t H_1^M = 2k_1 \left(\alpha_0 + \tfrac{1}{3}\tau k_2^2 H_2^M\right) H_1^M - 2\beta k_1^2 H_1^M - 2\nu_M k_1^2 H_1^M + \nabla \cdot \langle .. \rangle_1$$

$$\partial_t H_1^M + \partial_t H_2^M = -2\nu_M \left(k_1^2 H_1^M + k_2^2 H_2^M\right) + \nabla \cdot \langle .. \rangle_2$$

or

$$\partial_t H_2^M = -2k_1 \left(\alpha_0 + \tfrac{1}{3}\tau k_2^2 H_2^M\right) H_1^M + 2\beta k_1^2 H_1^M - 2\nu_M k_2^2 H_2^M + \nabla \cdot \langle . \rangle_2$$

(I used $k^2 \mathbf{A} \cdot \mathbf{B} = \mathbf{J} \cdot \mathbf{B}$ and assumed maximal helicity).

- MFD is **non-local** inverse cascade in this picture: transfer of magnetic helicity between small and large scales. In periodic box: no boundary terms.
- Can use these equations to explore different regimes of **fully dynamical mean field dynamo**, for example:

  1) steady-state and periodic boundaries

  2) time-dependent and periodic boundaries

  3) steady-state and open boundaries

  4) time-dependent and open boundaries

STEADY-STATE, PERIODIC BOUNDARIES

In steady-state, can write equation for small scale helicity as an equation for α:

$$\alpha = \frac{\alpha_0 + R_{M,2}\beta(\mathbf{B}\cdot\nabla\times\mathbf{B})/B^2}{1+R_{M,2}B^2/B_{eq}^2}$$

- Note Cattaneo & Hughes (1996) result for uniform $\overline{\mathbf{B}}$.
- For non-uniform $\overline{B}$, field evolution depends on $\overline{\mathbf{E}}\cdot\overline{\mathbf{B}}$. Assume $\beta=\beta_0$. We then have

$$\overline{\mathbf{E}}\cdot\overline{\mathbf{B}} = \alpha\overline{B}^2 - \beta\overline{\mathbf{B}}\cdot\nabla\times\overline{\mathbf{B}} = \frac{\alpha_0+R_{M,2}\beta_0\overline{\mathbf{B}}\cdot\nabla\times\overline{\mathbf{B}}/\overline{B}^2}{1+R_{M,2}\overline{B}^2/B_{eq}^2} - \beta_0\overline{\mathbf{B}}\cdot\nabla\times\overline{\mathbf{B}} = \frac{\alpha_0}{1+R_{M,2}\overline{B}^2/B_{eq}^2} + \frac{\beta_0}{1+R_{M,2}\overline{B}^2/B_{eq}^2}$$

- remarkable degeneracy: constant β emerges as the same as an artificially imposed symmetric, resisitive quenching of α and β.
- Current helicities are equal and opposite in steady state so in fact $\langle\mathbf{J}\cdot\overline{\mathbf{B}}\rangle \propto \alpha-\alpha_0$. This implies, for $\beta=\beta_0$, large R_m:

$$\alpha = \frac{\alpha_0}{1+\overline{B}^2\rangle/B_{eq}^2}$$

- for $\alpha\propto\beta$, one finds

$$\alpha = \frac{\alpha_0}{1+R_{M,2}(\alpha/\alpha_0+\overline{B}^2/B_{eq}^2-1)}.$$

- Determining actual value of α AND β even in steady-state is subtle.
- steady-state can be misleading for other reasons...

TIME-DEPENDENT AND PERIODIC BOUNDARIES

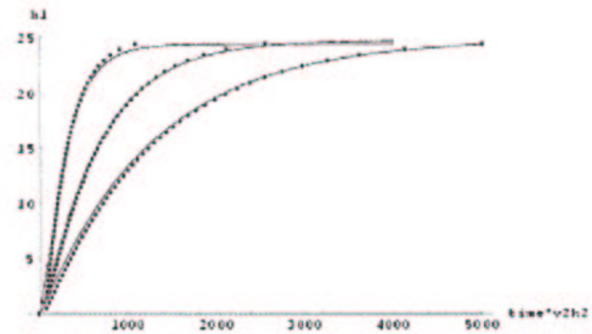

Figure 1: Solution for $h_1(t)$, $f_h=1$, $\beta\propto\alpha$. Here $k_2/k_1=5$ and the three curves from left to right have $R_M=100, 250, 500$ respectively. The dotted lines are quasi-empirical fits to Brandenburg 2001 for late times.

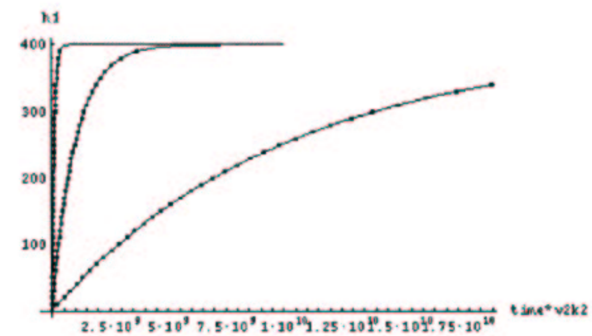

Figure 2: Solution for $h_1(t)$, $f_h=1$, $\beta\propto\alpha$. Here $k_2/k_1=20$ and the three curves from left to right have $R_M=10^7, 10^8, 10^9$ respectively.

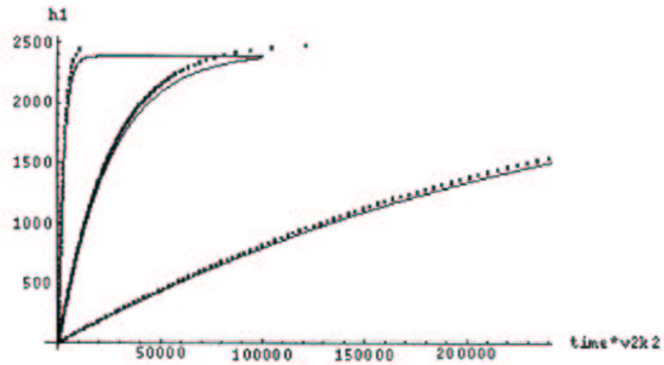

Figure 6: Solution for $h_1(t)$, $f_h = 1$, $\beta = \beta_0$. Here $k_2/k_1 = 50$ and the three curves from left to right have $R_M = 10^2, 10^3, 10^4$ respectively. The dotted lines are plotted from the formula used to quasi-empirically fit simulations of B01. For such large k_2/k_1 the fit to the data is only weakly sensitive to the form of β.

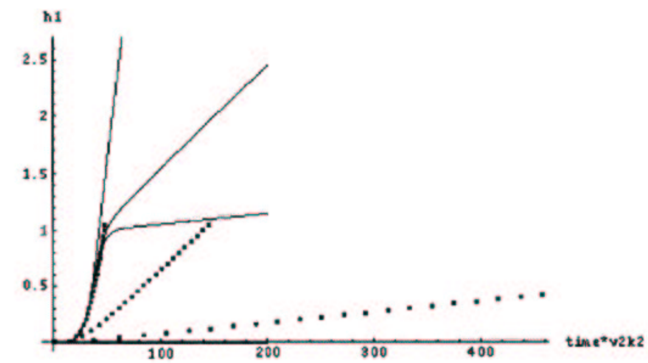

Figure 3: The early-time solution for $h_1(t)$, $f_h = 1$, $\beta \propto \alpha$. Here for $k_2/k_1 = 5$, and $R_M = 10^2, 10^3, 10^4$ from left to right respectively. Notice the significant departure from the formula of B01 at these early times. For $t < t_{kin}$ there is no dependence on R_M and the growth proceeds kinematically.

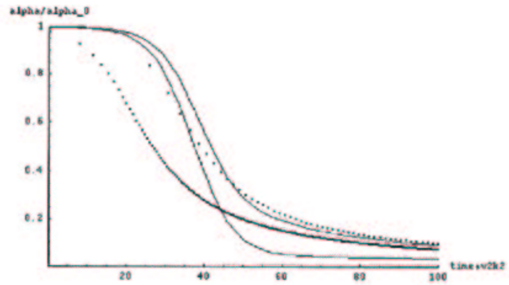

Figure 4: Solution of $\alpha/\alpha_0(t)$ for $h_1(t)$, $f_h = 1$, $\beta = \beta_0$. Here $k_2/k_1 = 5$ and the solid lines are our solutions for $R_M = 10^2$ (top curve) and $R_M = 10^3$ (bottom curve) respectively. The top and bottom dotted curves are interpreted from B01. Notice the longer kinematic phase for our solutions, the overshoot, and the convergence of the solution for $R_M = 10^2$ with that of the asymptotic quenching formula at $t = R_M$.

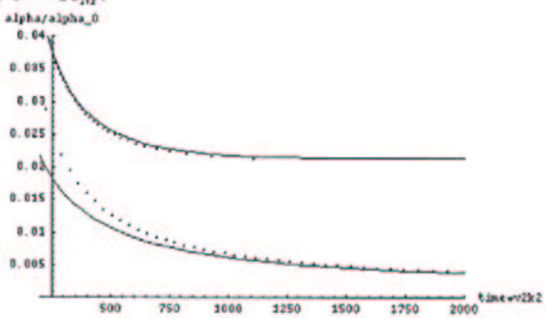

Fig. 5: This is the extension of Figure 4 for later times. Convergence of the $R_M = 10^3$ case to the asymptotic formula occurs at $t = R_M$.

Implications of the semi-analytic time-dependent solution for α^2 periodic box dynamo:

- Two scale approach works well for maximal forced helicity case.
- Mean field energy grows to $v_2^2 k_1/k_2$ independent of R_M on a few kinematic dynamo growth periods.
- R_M plays a role in dynamo coefficients after t_{kin} This agrees with B2001 simulations.
- Mean field saturates at $\overline{B}^2 = (k_2/k_1)b^2$ at $t \sim R_{M,1}k_2/k_1$.
- Value of saturated field strength implied by the "resistively limited" quenching formula is misleading for time-dependent theory.
- Need to worry next about boundary terms, and $\alpha - \Omega$ theory, and non-force free large scale fields.
- But simple case of α^2 seems to be understood in terms of helicity transfer.

BOUNDARY TERMS AND CORONAE/WINDS

- No periodic boundaries in nature (Ji99, BF00)
- Perhaps steady coronal flow of helicity & energy required for a FAST MFD
- $E_k \gtrsim kH_k$: flow of helicity to corona → energy flow to surface (BF01)
- Can estimate energy flow to surface for "steady" (on time scales longer than eddy turnover time) dynamo

$$dE/dt \gtrsim \alpha^2 \overline{\mathbf{B}}^2 R^2,$$

where $|\alpha| \sim |\tau_c \langle \mathbf{v} \cdot \nabla \times \mathbf{v} \rangle|$

- Coronal dissipation and variability is associated dynamo action
- Consistent with helicity and energy supply to Solar Corona, $\geq 10^{27}$erg/s.
- Predicts rate of energy supply into Galactic corona $\geq 10^{40}$erg/s.
- Consistent with inferred X-ray emission from AGN accretion disks ($\geq 10^{43}$erg/s),
- same physics may determine winds or jets that determines large scale field: Buoyancy, winds, etc.

"An open door may not be enough."

- Could jets, winds and dynamos be symbiotic?

GIF image 1000x989 pixels http://antwrp.gsfc.nasa.gov/apod/image/9903/scme_yohkoh_big.gif

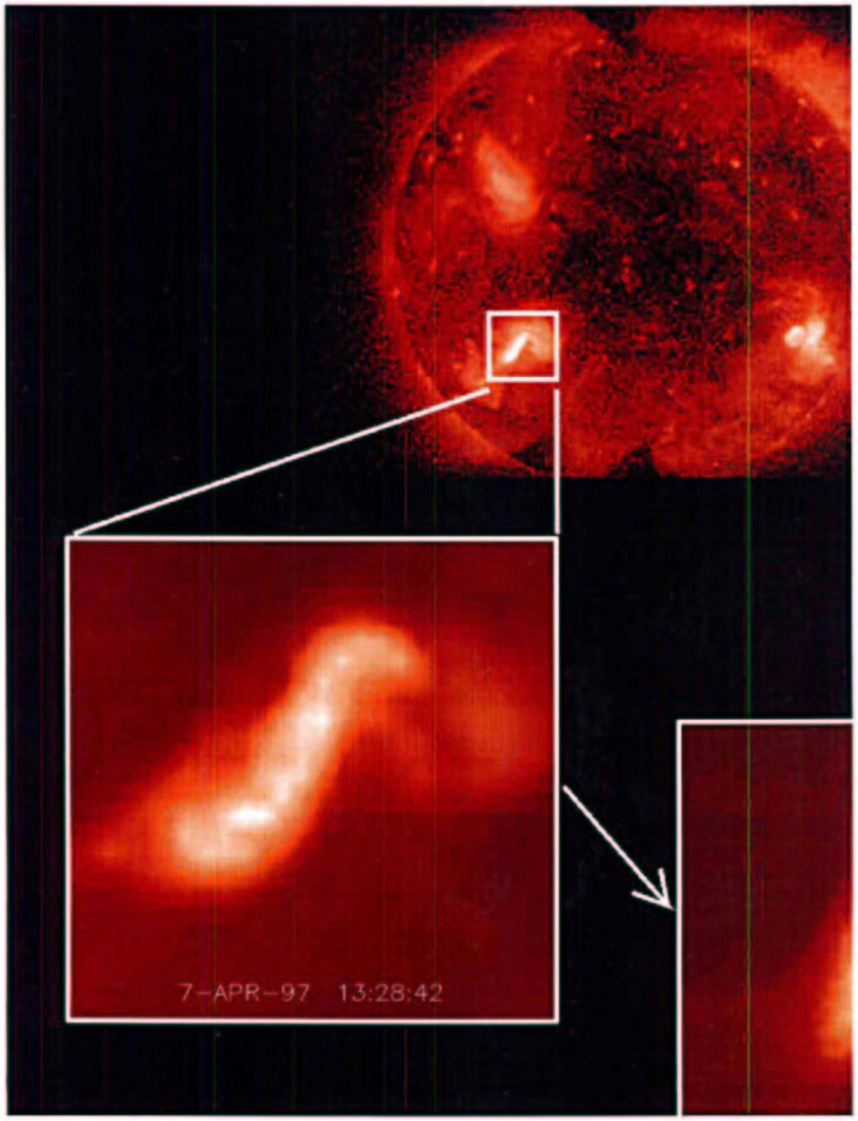

1 of 2 10/22/99 1:52 PM

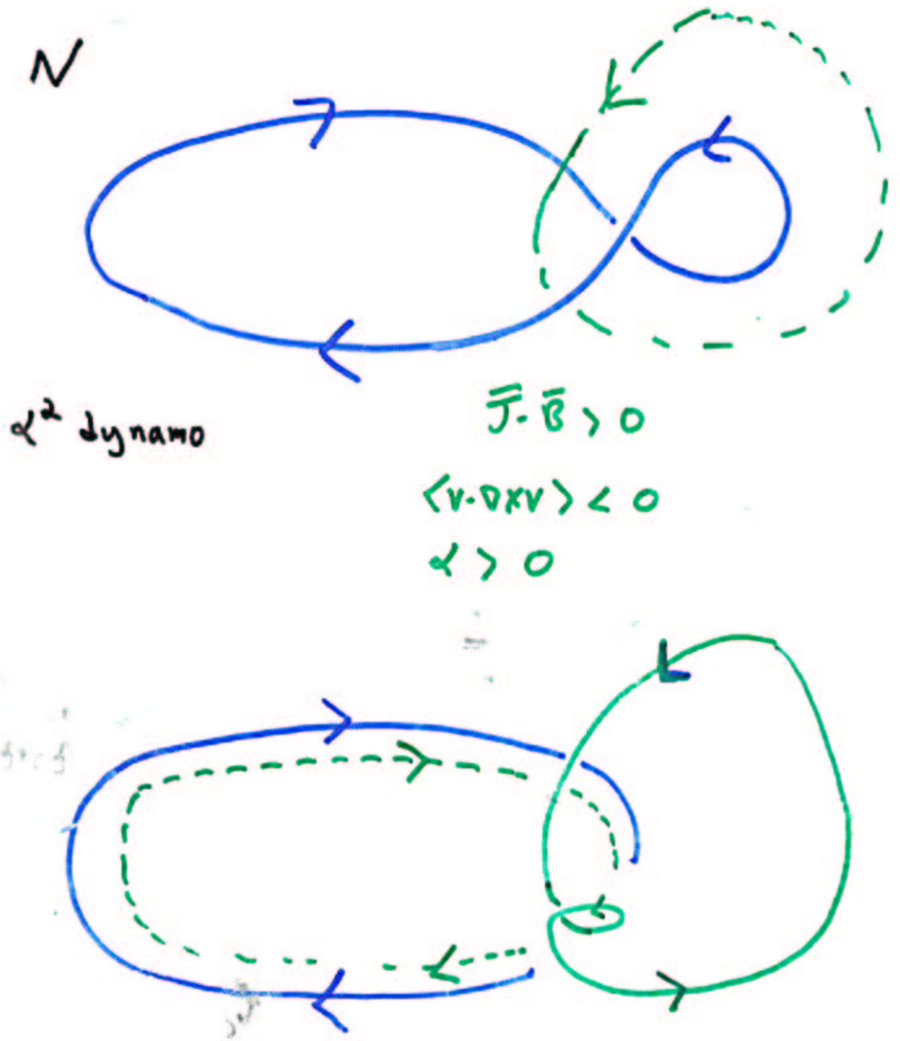

where is "small scale" $\langle j\cdot b\rangle$ of opposite sign to $\overline{J}\cdot\overline{B}$? Need to figure out with simple pictures!

WHAT ABOUT ZELDOVICH RELATION $\overline{B}^2 = b^2/R_m$?

• Catastrophic suppression "slow dynamo": would kill MFD in astrophysics

$$\alpha, \beta \simeq \frac{\alpha_{kin}, \beta_{kin}}{(1 + R_M\overline{\mathbf{B}}^2/\mathbf{b}^2)}$$

• Relation $\overline{\mathbf{B}}^2 = \mathbf{b}^2/R_m$ crops up now and then: **not** to be confused with quenching of dynamo!

• It originally came from interpreting 2-D Zeldovich (1957): fixed $\overline{\mathbf{B}}$, no bdry terms, asked **how large does $\mathbf{b}^2$ get**?

• $\partial_t\langle A_z^2\rangle = -\frac{\eta}{\delta^2(t)} < A_z^2 >= - < A_z^2 > /\tau_D$

• $\delta(t)$ marks scale of maximum magnetic energy.

• Kinematic regime: $d\delta/dt < 0$, τ_D, decreases as b energy grows.

• Kinematic regime ends when $b^2 = R_M\overline{\mathbf{B}}^2$, here τ_D is shortest and **small scale** field no longer grows.

• This is all irrelevant to 3-D dynamo since $\overline{B}$ cannot grow in this problem. In addition, b^2 would saturate at v_T^2 if the latter is smaller than $R_M\overline{B}^2$.

• We also saw that even in 3-D, when $\overline{B}$ is constant, the resistively limited dynamo coefficient can be misleading in estimating the actual field saturation value.

IMPLICATIONS OF EXISTING MFD QUENCHING RESULTS

- Dynamic non-linear semi-analytic theory of dynamo quenching agrees with numerical simulations for periodic box α^2 dynamo.
- Periodic b.c. are limited in two ways: They ignore the importance of boundary terms, but also allow strong rapid growth of a force-free field.
- More quenching studies with shear, stratification, and boundary terms are needed
- Currently there are no helical dynamo simulations which invoke astrophysically realistic boundary physics and stratification.

MOTION OF PEAK OF SMALL SCALE FIELD

- Motion of peak of **small scale** field energy represents **local** inverse cascade:
- take $k_m < k_n$ at which magnetic field dominates energy:

$$E_b(k_m) + E_b(k_n) = E_T(k_p)$$

$$H_b(k_m) + H_b(k_n) = E_b(k_m)/k_m + E_b(k_n)/k_n \leq E_T(k_p)/k_p$$

last inequality only satisfied if $k_p < k_n$

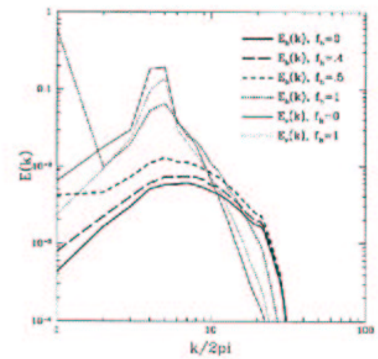

Figure 1: Saturated kinetic and magnetic energy spectra for values of f_h (MB 02).

The motion of the small scale peak is currently less well understood than the large scale field evolution.

- Effect of magnetic Prandtl number (mag. diffusivity/viscosity)

Conclusion/Discussion Points

• Inputting sufficient kinetic helicity into turbulence influences both the **large** and **small** scale magnetic spectrum. Growth of peak at forcing scale is *local* inverse cascade while growth of peak on large is a $non-local$ inverse cascade.

• Note role of *local* and $non-local$ inverse cascades, and *local* and $non-local$ direct cascades.

• **Large scale MFD as a "magnetic helicity transfer" process explains dynamical non-linear α^2 dynamo in a periodic box**. This is an important result and we need to build on this. How to apply to real system?

• α quenching vs. β quenching.

• **Does the same physics which determines winds, jets, coronae play a role in deteriming whether MFD dynamo is FAST or SLOW in real system?**

• Two-scale approaches are useful, particularly for helical turbulence.

• **Sheared Rotator** can provide "seed" in MFD framework, and can be also be source of turbulence, and stretching. MFD framework may apply to shear driven turbulence. How to fit in MRI.